

# Diffusive Dynamics of Vesicles Tethered to a Fluid Supported Bilayer by Single-Particle Tracking

Chiaki Yoshina-Ishii,<sup>†</sup> Yee-Hung M. Chan,<sup>†</sup> Joseph M. Johnson,<sup>†</sup> Li A. Kung,<sup>†</sup>  
Peter Lenz,<sup>‡</sup> and Steven G. Boxer<sup>\*,†</sup>

Department of Chemistry, Stanford University, Stanford, California 94305, and  
Department of Physics, Philipps-University Marburg, Renthof 5, D-35032 Marburg, Germany

Received December 17, 2005. In Final Form: April 13, 2006

We recently introduced a method to tether intact phospholipid vesicles onto a fluid supported lipid bilayer using DNA hybridization (Yoshina-Ishii, C.; Miller, G. P.; Kraft, M. L.; Kool, E. T.; Boxer, S. G. *J. Am. Chem. Soc.* **2005**, *127*, 1356–1357). Once tethered, the vesicles can diffuse in two dimensions parallel to the supported membrane surface. The average diffusion coefficient,  $D$ , is typically  $0.2 \mu\text{m}^2/\text{s}$ ; this is 3–5 times smaller than for individual lipid or DNA-lipid conjugate diffusion in supported bilayers. In this article, we investigate the origin of this difference in the diffusive dynamics of tethered vesicles by single-particle tracking under collision-free conditions.  $D$  is insensitive to tethered vesicle size from 30 to 200 nm, as well as a 3-fold change in the viscosity of the bulk medium. The addition of macromolecules such as poly(ethylene glycol) reversibly stops the motion of tethered vesicles without causing the exchange of lipids between the tethered vesicle and supported bilayer. This is explained as a depletion effect at the interface between tethered vesicles and the supported bilayer. Ca ions lead to transient vesicle–vesicle interactions when tethered vesicles contain negatively charged lipids, and vesicle diffusion is greatly reduced upon Ca ion addition when negatively charged lipids are present both in the supported bilayer and tethered vesicles. Both effects are interesting in their own right, and they also suggest that tethered vesicle–supported bilayer interactions are possible; this may be the origin of the reduction in  $D$  for tethered vesicles. In addition, the effects of surface defects that reversibly trap diffusing vesicles are modeled by Monte Carlo simulations. This shows that a significant reduction in  $D$  can be observed while maintaining normal diffusion behavior on the time scale of our experiments.

## 1. Introduction

We recently introduced a number of strategies for tethering lipid vesicles to a supported lipid bilayer using DNA hybridization as illustrated schematically in Figure 1.<sup>1,2</sup> We envision this system as a useful method for creating two-dimensional arrays of integral membrane proteins in vesicles and as a platform for studying their interactions with other proteins, small molecules, and/or vesicles. Fluid supported lipid bilayers are first prepared by vesicle fusion to a cleaned glass substrate using vesicles that display short oligonucleotides (sequence A') on their surfaces. Subsequently, fresh vesicles displaying the complementary oligonucleotide (denoted A) are flowed over the planar supported bilayer leading to sequence-specific tethering of these intact vesicles to the supported bilayer. Tether lengths of 16- to 24-mers and extruded vesicle sizes ranging from 30 to 200 nm were successfully used (lengths and sizes outside these ranges have not yet been tested).<sup>3</sup> The system is also compatible with a wide range of lipid compositions, and the supporting bilayer and tethered vesicle compositions are independently variable. Several laboratories have used biotinylated lipid headgroups and streptavidin to tether vesicles to supported membranes.<sup>4</sup> In our hands, these tethered vesicles are not reproducibly laterally mobile, and

this tethering system does not allow for the possibility of sequence-encoded tethering, for example, to prepare vesicle arrays.<sup>1,2</sup> A cholesterol–DNA conjugate, used in pairs, can also be used to tether vesicles,<sup>5</sup> and bulk measurements of their diffusion using fluorescence recovery after photobleaching (FRAP) have been reported.<sup>6</sup>

Individual vesicles are easily visualized by adding either leaflet or content fluorescent labels and by using epifluorescence microscopy. Tethered vesicles are observed to diffuse in the plane parallel to the supported bilayer and reversibly collide. (See movie 1, Supporting Information. Note that this article focuses on dynamic processes, and many of the effects are best seen by video microscopy. Quantitative analysis is based on single-particle tracking.<sup>1</sup>) The dependence of this diffusion under collision-free conditions on the properties of the system is described in the following text. We find that the lateral diffusion coefficient for tethered vesicles is independent of their size and bulk viscosity in the range studied but that the average diffusion coefficient is 3 to 5 times slower than for lipids or lipid-anchored double-helical DNA in the supporting membrane. Possible origins for this reduction are described and either tested or modeled. In particular, we focus on two perturbations that greatly affect diffusion and can be visualized only by single-particle tracking: the effects of the addition of macromolecules such as PEG and the effects of added Ca ions when negatively charged lipids are present in both the tethered vesicle and the supporting bilayer. These effects are both interesting and useful in their own right and provide insight into possible frictional coupling between the tethered vesicle and the supporting bilayer. Collisions with sticky defects are also documented, and modeling shows that they could affect the average diffusion as well. The diffusive properties of

\* Corresponding author. E-mail: sboxer@stanford.edu. Tel: (650) 723-4482. Fax: (650) 723-4817.

<sup>†</sup> Stanford University.

<sup>‡</sup> Philipps-University Marburg.

(1) Yoshina-Ishii, C.; Boxer, S. G. *J. Am. Chem. Soc.* **2003**, *125*, 3696–3697.

(2) Yoshina-Ishii, C.; Miller, G. P.; Kraft, M. L.; Kool, E. T.; Boxer, S. G. *J. Am. Chem. Soc.* **2005**, *127*, 1356–1357.

(3) 24-mer oligonucleotide tethers were used in this study. The sequences used were either 5'-TAG TAT TCA ACA TTT CCG TGT CGA-3' and its conjugate or 5'-TGC GGA TAA CAA TTT CAC ACA GGA-3' and its conjugate.

(4) For examples, see (a) Boukobza, E.; Sonnenfeld, A.; Haran, G. *J. Phys. Chem. B* **2001**, *105*, 12165–12170. (b) Okumus, B.; Wilson, T. J.; Lilley, D. M.; Ha, T. *Biophys. J.* **2004**, *187*, 2798–2806.

(5) Pfeiffer, I.; Höök, F. *J. Am. Chem. Soc.* **2004**, *126*, 10224–10225.

(6) Benkoski, J. J.; Höök, F. *J. Phys. Chem. B* **2005**, *109*, 9773–9779.

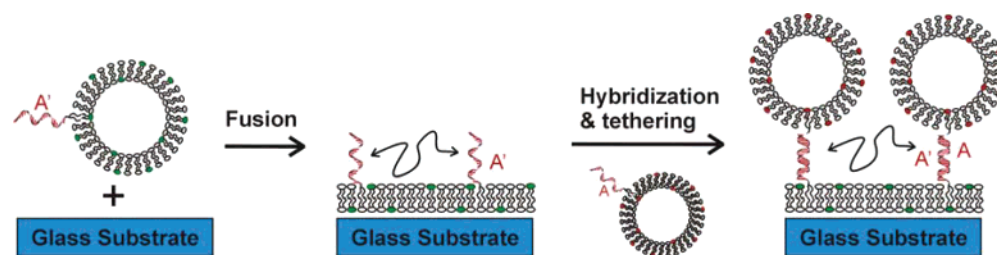


**Figure 1.** Schematic of the tethered vesicle assembly process. Vesicles displaying oligonucleotide with sequence  $A'$  are exposed to a cleaned glass substrate to form a supported bilayer displaying mobile (indicated with the double arrow) oligonucleotides on the surface. Subsequent incubation with fresh vesicles displaying oligonucleotide with complementary sequence  $A$  results in the assembly of mobile tethered vesicles by hybridization and tethering.

these complex self-assembled objects are intrinsically interesting, and understanding their diffusion is important for their application to studies of vesicle–vesicle interactions at the level of individual vesicles. The effects of applied electric fields on the motion of tethered vesicles,<sup>1,7</sup> vesicle–vesicle interactions visualized for individual vesicles, and tethered proteoliposomes will be described in subsequent manuscripts.

## 2. Materials and Methods

**2.1. Vesicle Preparation.** In a typical experiment, a mixture of lipids containing 5 mg of egg phosphatidylcholine (egg PC, Avanti Polar Lipids) and 90  $\mu\text{g}$  (1 mol %) of fluorescently labeled lipid, Texas Red 1,2-dihexadecanoyl-*sn*-glycero-3-phosphoethanolamine (TR-DHPE, Molecular Probes) in chloroform was dried to a film and reconstituted in PBS buffer (10 mM phosphate, 100 mM NaCl, pH 7.2) to 10 mg/mL. The lipid mixture was extruded through a 100 nm polycarbonate membrane (Avanti) to form small unilamellar vesicles. A 100 nm vesicle containing 1 mol % of Texas Red lipids has about 1000 fluorophores/vesicles and is easily visualized by using epifluorescence microscopy. Lipophilic oligonucleotide ( $C_{18}$ )<sub>2</sub>- $A'$ <sup>2,3</sup> was dissolved in 1:1 acetonitrile/water to a concentration of 10  $\mu\text{M}$ . The ( $C_{18}$ )<sub>2</sub>- $A$  solution (0.6  $\mu\text{L}$ , on average 0.1 DNA/vesicle) was added to the vesicles prepared above at room temperature while mixing and incubated at 4  $^{\circ}\text{C}$  for 3 h. Similarly, vesicles used to form the supporting bilayer were made using 5 mg of egg PC, 115  $\mu\text{g}$  of 1-palmitoyl-2-[12-[(7-nitro-2-1,3-benzoxadiazol-4-yl)amino]-dodecanoyl]-*sn*-glycero-3-phosphocholine (NBD-PC, 2 mol %, Avanti Polar Lipids), and 101  $\mu\text{g}$  of 1,2-dipalmitoyl-*sn*-glycero-3-[phospho-L-serine] (DPPS, 2 mol %, Avanti Polar Lipids). A 10  $\mu\text{M}$  ( $C_{18}$ )<sub>2</sub>- $A'$  solution (6  $\mu\text{L}$ ) was added to these vesicles to yield vesicles with an average number of one  $A'$  DNA per vesicle. Using similar procedures, vesicles for tethering with average diameters of 30, 100, and 200 nm were prepared, and the average number of DNAs displayed on the tethered vesicle was varied from 0.1/vesicle to 25/vesicle.

Supported bilayers displaying oligonucleotides are formed by vesicle fusion onto a cleaned glass coverslip as described earlier for simple lipids<sup>8</sup> by adding 35  $\mu\text{L}$  of vesicles displaying ( $C_{18}$ )<sub>2</sub>- $A'$  and are labeled with NBD-PC diluted to 2 mg/mL in a CoverWell perfusion chamber gasket (9 mm diameter, 0.5 mm thickness, Molecular Probes) and rinsing with buffer after a 15 min incubation period. Vesicles (4  $\mu\text{L}$ ) displaying ( $C_{18}$ )<sub>2</sub>- $A$  and labeled with TR-DHPE are injected into the gasket and mixed. After a 45 min incubation period at room temperature, the gasket is thoroughly washed with buffer, and tethered vesicles are observed with a Nikon TE300 inverted epifluorescence microscope and a 100X oil-immersion objective.

**2.2. Macromolecule and Ca Ion Perturbations.** The effects of macromolecules such as poly(ethylene glycol) (PEG) were studied by flowing a buffered solution of the macromolecule over the surface using a simple two-lane microfluidic system similar to that described by Kam and Boxer.<sup>9</sup> In this way, the effects of added polymers on

a population of tethered vesicles can be compared directly with a control population that is exposed to hydrodynamic flow but no macromolecule or  $\text{Ca}^{2+}$ . PEG 8000 was obtained from J. T. Baker. The effects of Ca ions on tethered vesicle–tethered vesicle interactions and on tethered vesicle–supported bilayer interactions were measured by including DPPS in the tethered vesicles alone, the supported bilayer alone, or the tethered vesicle and supported bilayer. Vesicles for  $\text{Ca}^{2+}$  experiments were formed in Tris (10 mM Tris pH 8, 100 mM NaCl) or HEPES buffer (10 mM HEPES pH 7.2, 100 mM NaCl) to avoid the precipitation of calcium phosphate.  $\text{Ca}^{2+}$  was introduced using the same buffers plus 10 mM  $\text{CaCl}_2$ .

**2.3. Single-Particle Tracking Analysis Parameters.** The 2D diffusive motions of vesicles are visualized by video microscopy at rates varying from 36 to 100 ms/frame for 100 frames. Vesicle trajectories were tracked using Metamorph's motion analysis and particle tracking plug-in software (version 6.1r0, Universal Imaging). Mean square displacements (MSDs) at defined time intervals,  $\Delta t$ , were calculated using unweighted internal averaging over all time pairs.<sup>10</sup> Least-squares fits of the MSD versus time interval plots were calculated up to the 15th time interval. Particles that showed a nonlinear relationship between MSD and time ( $R^2 < 0.97$ ) and particles that appear to collide with one another were rejected from further analysis. (See the comments at end of the next paragraph.) Diffusion properties of individual vesicles can be analyzed by single-particle tracking and analysis methods.<sup>10,11</sup> The MSD for every time interval is calculated from

$$\text{MSD}(\Delta t) = \langle (x_{i+n} - x_i)^2 + (y_{i+n} - y_i)^2 \rangle \quad (1)$$

$$n = 1, 2, 3, \dots, (N_T - 1)$$

where a vesicle at position  $(x_i, y_i)$  moves to position  $(x_{i+n}, y_{i+n})$  after a time interval  $\Delta t = n \times$  (video frame time).  $N_T$  is the total number of steps recorded, and for a particular  $n$ ,  $i$  ranges from 1 to  $N_T$  to  $n$ .

For a randomly diffusing particle in two dimensions, the trajectory is described by

$$\text{MSD}(\Delta t) = 4D\Delta t \quad (2)$$

where  $D$  is the diffusion coefficient. The distribution is characterized by the standard deviation,  $\sigma$ , of diffusion coefficients for such objects and can be estimated by<sup>12</sup>

$$\sigma = D \left[ \frac{2N_D}{3(N_T - N_D)} \right]^{1/2} \quad N_D \ll N_T \quad (3)$$

where  $N_T$  is the total number of steps observed and  $N_D$  is the time interval over which the least-squares fit to the data is performed. For the analysis of all experimental and simulated trajectories in this article,  $N_T = 100$  and  $N_D = 15$ . The source of nonrandom or

(10) Saxton, M. J. *Biophys. J.* **1997**, *72*, 1744–1745.

(11) Saxton, M. J.; Jacobson, K. *Annu. Rev. Biophys. Biomol. Struct.* **1997**, *26*, 373–399.

(12) (a) Saxton, M. J. *Biophys. J.* **1997**, *72*, 1744–1753. (b) Qian, H.; Sheetz, M. P.; Elson, E. L. *Biophys. J.* **1991**, *60*, 910–921.

(7) Yoshina-Ishii, C.; Boxer, S. G. *Langmuir* **2006**, *22*, 2384–2391.

(8) Groves, J. T.; Boxer, S. G. *Acc. Chem. Res.* **2002**, *35*, 149–157.

(9) Kam, L.; Boxer, S. G. *J. Am. Chem. Soc.* **2000**, *122*, 12901–2.

anomalous diffusion for vesicles that exhibit nonlinear MSD versus time plots is not known; possibly related behavior has been described in SPT measurements on fluorescent lipids in supported bilayers.<sup>17</sup> The most common deviation was negative curvature, and even then most could be fit with a straight line with  $R^2 > 0.90$ . The selection of vesicles that exhibit truly random diffusion with  $R^2 > 0.97$  thus tends to reject trajectories that would give an artificially low  $D$  by our analysis. Even so, the average  $D$  for tethered vesicles is considerably slower than for lipids in supported bilayers, as described in detail in section 3.1.

**2.4. Lattice Model of Diffusion.** We modeled the diffusive motion of vesicles using 1000 random walkers on a square lattice with  $1000 \times 1000$  sites. In every iteration, all random walkers randomly pick a step direction (where the directions up, down, left, and right all have the same probability) and then move one lattice site in this direction provided that the target lattice site is free. If the lattice site is occupied by another vesicle, then this event is interpreted as a collision between the two vesicles. The initial configuration is random, and periodic boundary conditions are used (i.e., a vesicle that steps over the boundary reenters the system on the opposite side).

In the limit of small densities of vesicles (where the number of collisions is small), the movement of the random walkers is characterized by a diffusion coefficient

$$D_m = \frac{\Delta x^2}{4\Delta t}$$

where  $\Delta x$  is the distance a vesicle typically moves in the time interval  $\Delta t$ . In the simulations,  $\Delta x$  is the lattice spacing, and  $\Delta t$  is the time between two hopping events. In the following text, all diffusion coefficients  $D$  will be measured in units of  $D_m$ . Thus, the lattice spacing has unit length (in units of  $\Delta x$ ), and an iteration step corresponds to a time interval of length  $\Delta t$ .

The trajectories of all particles are tracked for 100 steps. With the same methods as described above for the analysis of experimental diffusion trajectories (section 2.2), the diffusion coefficient  $D$  of the random walkers can be determined by fitting the 15-step MSDs with a line of slope  $4D$ . In accordance with the analysis of the experimental data, only those vesicle trajectories are analyzed that neither step out of the system nor collide with other trajectories.

The simulations can also be used to model the influence of sticky defects on the diffusion coefficients of vesicles tethered to supported bilayers. Such defects can be modeled as transient traps for random walkers. In the simulations, these traps are implemented by assigning escape probabilities  $p_e$  to all lattice sites. Thus, a random walker at site  $i$  will try to move away from this site only with probability  $p_e$ . In the simulations, the walker tries to move only if a randomly picked number  $0 \leq p \leq 1$  fulfills  $p < p_e(i)$ . Defect-free lattice sites have  $p_e = 1$  whereas for traps  $p_e = p_t = 0.1$ . Here, we consider only systems where all traps are characterized by the same  $p_t$ . This procedure is equivalent to assigning a diffusion coefficient  $D_t = p_t D < D$  to the traps. In the following text, we systematically vary the defect density. Diffusion coefficients are determined by averaging over  $N_r$  independent runs.

(13) Metamorph's particle-tracking algorithm looks for the translation of the initial shape and intensity profile of a particle inside a small box from frame to frame. When photobleaching changes the apparent shape and size of the particle, the position determination becomes less accurate.

(14) Fein, M.; Unkeless, J.; Chuang, F. Y. S.; Sassaroli, M.; Costa, R.; Väänänen, H.; Eisinger, J. *J. Membr. Biol.* **1993**, *135*, 83–92.

(15) Lee, G. M.; Ishihara, A.; Jacobson, K. A. *Proc. Natl. Acad. Sci. U.S.A.* **1991**, *88*, 6274–6278.

(16) Lee et al.<sup>15</sup> tracked 40 nm gold particles that were bound to a supported membrane using antibodies. It was observed that even in the limit where only one antibody anchor was expected to tether the gold particle single-particle tracking yielded diffusion coefficients that were, on average, a factor of 2 smaller than lipid diffusion coefficients. Changing the viscosity of the medium by the addition of glycerol to 30% did not affect  $D$ . When diffusion was measured by SPT in the case where multiple tethers were expected,  $D$  was further decreased.

(17) Schmidt, Th.; Schütz, G. J.; Baumgartner, W.; Gruber, H. J.; Schindler, H. *J. Phys. Chem.* **1995**, *99*, 17662–17668.

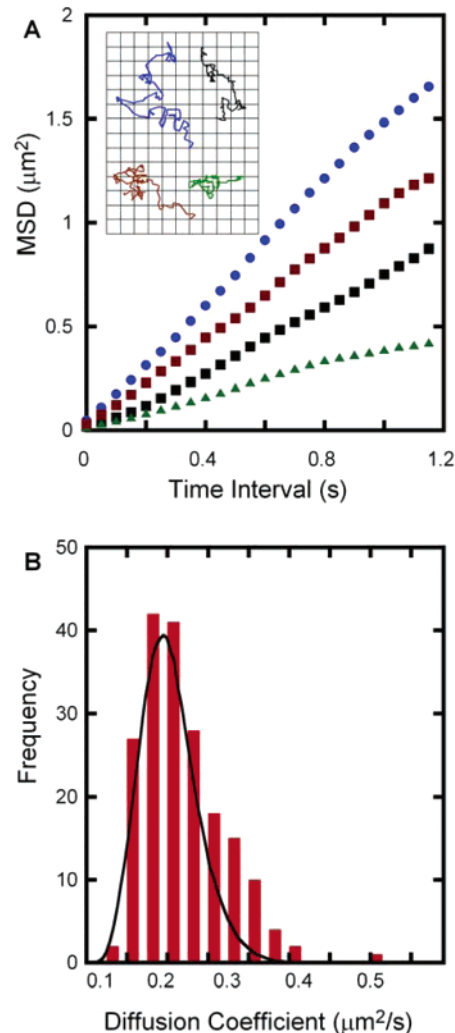


**Figure 2.** (A) Mean square displacement versus time plots of the four example trajectories in the inset showing a linear relationship as expected from a random walk trajectory. The diffusion coefficients are  $0.37$  (blue),  $0.27$  (red),  $0.19$  (black), and  $0.10 \mu\text{m}^2/\text{s}$  (green). The grid in the inset is  $0.5 \mu\text{m} \times 0.5 \mu\text{m}$ , and the total time interval is  $3.6$  s. (B) Histogram plot of 190 independent vesicle diffusion coefficients with an average value of  $0.2 \mu\text{m}^2/\text{s}$ . The black curve is the statistically predicted width of the distribution for this average value (eq 3).

### 3. Results and Discussion

**3.1. Diffusion of Tethered Vesicles by Single-Particle Tracking.** The trajectories taken by four typical 100 nm tethered vesicles are shown in the inset of Figure 2A; their corresponding MSD versus time plots, analyzed using unweighted internal averaging over all time pairs, are shown in Figure 2A. As expected, linear relationships are observed for most particles, and diffusion coefficients can be extracted. The criteria for rejecting nonlinear plots were discussed in section 2.3. Figure 2B shows a histogram plot of 190 independent vesicle diffusion coefficients, where the black curve is the statistically predicted distribution for this experiment (eq 3, ref 12). The tethered vesicles were modified with an approximately 0.1 equivalent of  $(\text{C}_{18})_2\text{-A}'$  DNA relative to vesicles. Under these conditions, it is expected that vesicles should have at most one DNA/vesicle and that those that tether should have exactly one DNA because most vesicles have no DNA; these are not tethered and are not observed (discussed further below). The average diffusion coefficient for this set of trajectories is  $0.2 \mu\text{m}^2/\text{s}$ . Typical mean diffusion coefficients vary from  $0.2$  to  $0.4 \mu\text{m}^2/\text{s}$  with standard deviations ranging

from about 0.15 to 0.25  $\mu\text{m}^2/\text{s}$ . The expected statistical spread of diffusion coefficients is given by eq 3, which corresponds to 0.07 to 0.1  $\mu\text{m}^2/\text{s}$  in our experiments; however, there are other experimental sources of error that will add to the uncertainty in the measurement of  $D$ . The mechanical stability of the apparatus and the ability of the particle-tracking algorithm to track vesicles accurately with a changing intensity profile due to photobleaching and motion during exposure make significant contributions to the experimental error. For a particle with a diffusion coefficient of 0.4  $\mu\text{m}^2/\text{s}$  and an exposure time of 36 ms, the length scale of motion is 0.24  $\mu\text{m}$  or over 3 pixels at 100 $\times$  magnification with our apparatus. Because vesicle images typically cover  $5 \times 5$  to  $10 \times 10$  pixels, this is a significant contribution. In addition, because the integrated fluorescence intensity of an individual vesicle decreases by 10–50% during a typical video acquisition, accurate position determination is a challenge.<sup>13</sup> Thus, we expect that the observed distribution of  $D$  should be larger than that predicted by statistical analysis alone.

The diffusion coefficient of NBD-PC in the supporting bilayer was measured by fluorescence recovery after photobleaching (FRAP) and determined to be  $1.4 \pm 0.2 \mu\text{m}^2/\text{s}$ , which shows that the tethered vesicles do not affect the diffusion of lipids in the bilayer. To determine if double-helical DNA contributes to the reduced diffusion coefficient, a supporting bilayer was prepared displaying DNA with sequence A' and also containing a lipid label, NBD-PE (2 mol %); this surface was incubated with complementary DNA sequence A conjugated to Cy5 fluorophore on the 5' end. FRAP experiments on NBD and Cy5 gave diffusion coefficients of  $1.2 \pm 0.2$  and  $1.3 \pm 0.3 \mu\text{m}^2/\text{s}$ , respectively, showing that the double-helical DNA alone is not responsible for the observed reduction in the diffusion coefficient of tethered vesicles compared with membrane lipids.

Single-particle tracking (SPT) is a method that samples a shorter time and smaller area than FRAP, which measures an average diffusion coefficient over many molecules. Therefore, the two measurements of  $D$  are not necessarily the same. Saxton and Jacobson<sup>11</sup> summarize SPT and FRAP measurements in membranes reported in the literature. It is evident that the nature of the label and details of the system sometime cause very large discrepancies between the two measurements. In cases where colloidal gold probes or fluorescent beads were used to track the diffusion of lipids in a supported bilayer,<sup>14,15</sup> diffusion was 2–4 times smaller compared to FRAP measurements without colloidal probes.<sup>16</sup> In contrast, when individual rhodamine-labeled lipid analogues were tracked, FRAP and SPT give much better agreement, with SPT values being slightly higher.<sup>17</sup> In our experiments, diffusion coefficients measured for DNA-tethered vesicles are consistently smaller by a factor of 3–5 compared to diffusion coefficients measured by FRAP for fluorescent labels in supported membranes. (See the comments at end of section 2.3.)

To test possible mechanisms for the reduction in  $D$  for tethered vesicles relative to lipid components, a series of experiments were performed. First, vesicles were extruded through polycarbonate membranes with pore sizes varying from 30 to 200 nm, and their diffusion was analyzed by SPT. As shown in Figure 3A, for the size range that was studied, no correlation between the extruded size and the average diffusion coefficient from SPT was observed. These observations were corroborated by a related experiment where the inherent size distribution of extruded vesicles was exploited. Vesicles extruded through 100 nm membranes have a standard deviation for the diameter distribution

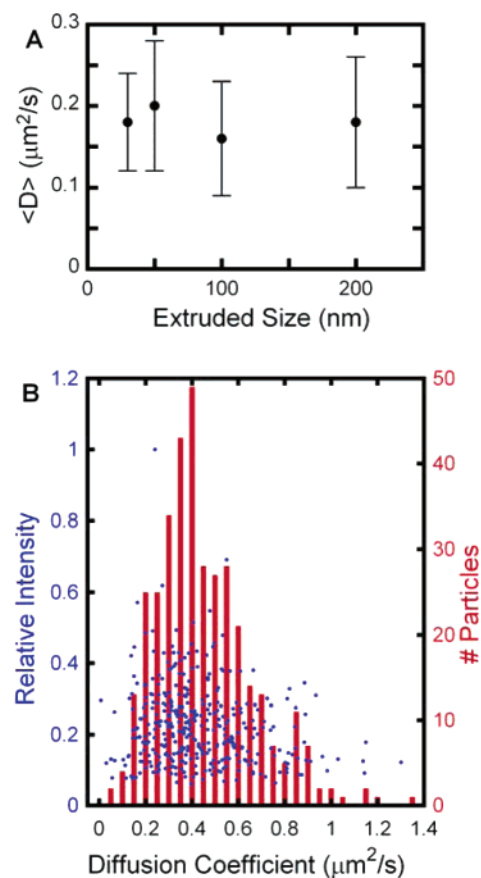


**Figure 3.** (A) Measured average diffusion coefficients of tethered vesicles as a function of extruded size between 30 and 200 nm. In this range, no dependence of size on  $D$  was observed. (B) Vesicles extruded through 100 nm polycarbonate membranes were tethered, and diffusion coefficients were measured with a distribution shown in the histogram in red. The intensity variation of the individual vesicles under epifluorescence microscopy reflects the intrinsic size distribution of extruded vesicles. Relative integrated intensities for each vesicle were plotted against their diffusion coefficients (blue). No correlation between intensity and diffusion coefficient was observed, consistent with the observation in A.

of greater than 10%.<sup>18</sup> This is reflected in the intensity variation for different tethered vesicles under an epifluorescence microscope. As shown in Figure 3B, when the relative integrated intensities (blue dots) of vesicles are plotted against their diffusion coefficients no correlation is found, consistent with the observations on collections of vesicles whose sizes are, on average, different (Figure 3A). In a separate experiment, vesicle diffusion was studied as a function of bulk aqueous viscosity, achieved by increasing amounts of glycerol from 0 to 30% vol/vol. It was found that vesicle diffusion was independent of up to 3-fold changes in bulk viscosity.

Although these experiments suggest that the diffusive property of tethered vesicles is controlled by the viscous, hydrophobic part of the membrane where the viscosity is 2 to 3 orders of magnitude higher than for water, the observed diffusion coefficient is lower than for the lipids or lipid-anchored DNA in the supporting bilayer. In the following text, we consider possible origins of this reduction, focusing on multiple tethers, interactions between tethered vesicles and the supported bilayer, and sticky defects on the surface.

(18) (a) Korgel, B. A.; van Zanten, J. H.; Monbouquette, H. G. *Biophys. J.* **1998**, *74*, 3264–3272. (b) Hallett, F. R.; Watton, J.; Krygsman, P. *Biophys. J.* **1991**, *59*, 357–362.

There is no obvious direct assay for the number of tethers associated with each vesicle, so we base our analysis on the expected effect of multiple tethers on tethered vesicle diffusion. Both the free area and hydrodynamic models of lipid diffusion suggest that as the radius of an integral membrane component increases the diffusion coefficient should decrease.<sup>19</sup> Although a single membrane-associated region of the DNA–lipid conjugate is similar in size to a single lipid, there is the possibility of forming multiple anchors between the vesicle and the supporting bilayer, effectively increasing the radius of the membrane-bound component, and this would be expected to reduce the diffusion coefficient. The histograms in Figures 2 and 3 are diffusion coefficients measured for vesicles tethered on a supported bilayer where, on average, 0.1 DNA–lipid molecule was added for every vesicle. Under these conditions, it is expected that vesicles should have at most one DNA displayed (assuming Poisson statistics, 0.45% of vesicles would have 2 DNA-lipids); most will not tether because they have no DNA displayed on their surface, and those that do tether should have exactly one DNA. An experiment was performed where an average of 25 DNA molecules were added per 100 nm vesicle. (It was demonstrated previously that multiple DNA–lipid conjugates efficiently insert into vesicles.<sup>2</sup>) Under these conditions, we would expect that multiple tethering could occur and that if multiple tethering occurs it would reduce the diffusion coefficient. The measured diffusion coefficients of these tethered vesicles by SPT were indistinguishable from those of tethered vesicles where at most one tether was used (data not shown), suggesting that multiple tethering does not occur.<sup>20</sup> Although we cannot rule out the possibility that the addition of DNA–lipid to vesicles does not occur statistically, creating a population of vesicles with multiple DNA strands displayed on the surface even in the case of 0.1 DNA/vesicle, which then tether preferentially to the surface, the experimental results are consistent with the scheme in Figure 1 where only one tether is required. The small vesicles used in these experiments have high curvature, and it may not be possible for multiple DNA tethers to form without severely straining the vesicle and bringing the tethers into close contact. Tethering of giant ( $> 1 \mu\text{m}$ ) vesicles will be described in subsequent papers.

**3.2. Effects of Macromolecules on Tethered Vesicle Diffusion.** As part of ongoing studies of interactions between tethered vesicles, the effect of PEG 8000 was studied. PEG has been shown to enhance vesicle–vesicle interactions and even cause fusion for certain lipid compositions in bulk suspensions of vesicles.<sup>21</sup> Immediately upon addition of buffer containing PEG 8000 at concentrations that do not cause irreversible aggregation or fusion between bulk and tethered vesicles, tethered vesicles were observed to stop moving. This effect can be visualized by using a two-lane microfluidic device where 5% w/v PEG 8000-containing buffer is flowed over one-half of the tethered vesicles (100 nm, 1% TR-DHPE) in the microscope field of view and PEG-free PBS buffer is flowed over the other half. (See movie 2 in Supporting Information.) In the lane with PEG-free PBS

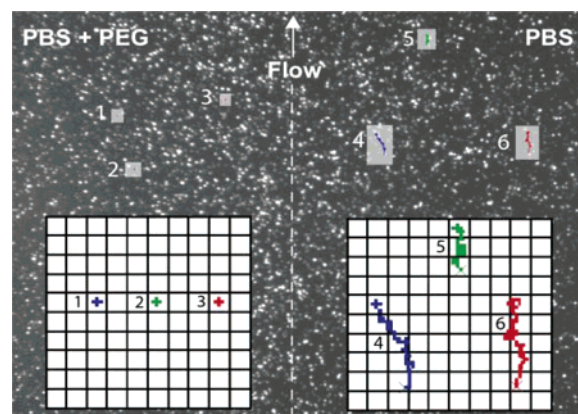


**Figure 4.** Trajectories of tethered vesicles in a two-lane microfluidic device. Tethered vesicles were deposited in the device. Then PBS was flowed on the right half, and PBS + PEG was flowed on the left half with the direction of flow proceeding from the bottom to the top of the image. The dashed line marks where the two lanes meet. Trajectories of the selected vesicles were recorded for frames 300–350 from movie 3 (Supporting Information), overlaid on frame 300, and magnified in the insets with the initial positions of the vesicles marked with an x.

buffer, vesicles exhibit biased motion in the direction of hydrodynamic flow as well as diffusional motion. In the lane with PBS containing PEG, most vesicles do not respond to flow, and diffusion stops virtually completely. When monitored over long periods of time, very slow diffusion of these vesicles can still be detected. Figure 4 shows representative trajectories in the two lanes and illustrates the reduced mobility of the vesicles upon exposure to PEG. Removing PEG by washing with PBS restores vesicle mobility. SPT analysis of tethered vesicles before introducing PEG and after washing PEG away under nonflow conditions shows that  $D$  is unchanged by the process. Note that the bulk viscosity of the solution is 4 to 5 times that of water but that changes in the bulk viscosity to a similar level by the addition of glycerol had no effect on vesicle diffusion. The diffusion of lipid-conjugated fluorophores in the supported bilayer is unaffected by the addition of PEG. No fusion of tethered vesicles is observed at the concentration of PEG studied here. Furthermore, there is no evidence of mixing between the lipids in the supporting bilayer and the tethered vesicles when PEG is added. This could be observed by including a dye in the tethered vesicles but not the supporting bilayer; no loss of dye from the tethered vesicles to the supporting bilayer was observed when vesicles were incubated for hours with PEG (data not shown). Alternatively, lipids that may be exchanged in the presence of PEG between the supporting membrane and vesicles can be sensitively detected by labeling the supporting bilayer but not the tethered vesicles and then, after incubation with PEG, using an electric field applied parallel to the substrate to separate the dye in the supporting membrane and tethered vesicles.<sup>1,7</sup> This method cleanly separates the tethered vesicles from dye in the supporting bilayer so that vesicles that may have picked up only a few dye molecules can be sensitively detected (ref 1 in Supporting Information and ref 7), but dye was not detected in them (data not shown).

The most likely explanation for this behavior is that the introduction of a low concentration of polymer gives rise to a depletion effect.<sup>22,23</sup> Because polymer molecules cannot pass through the lipid bilayers of tethered vesicles or of supported

(19) Vaz, W. L. C.; Goodsaid-Zalduendo, F.; Jacobson, K. *FEBS Lett.* **1984**, *174*, 199–207.

(20) Benkowski and Höök have measured the diffusion of single cholesterol-anchored DNA-tethered vesicles by FRAP and have obtained a diffusion coefficient of  $0.3 \mu\text{m}^2/\text{s}$  (Benkowski, J. J.; Höök, F. *J. Phys. Chem. B*, in press, 2005). As a variation of the tether where a double cholesterol anchor was used, the observed diffusion coefficient decreased to  $0.1 \mu\text{m}^2/\text{s}$ . In the single cholesterol-anchored case, the binding to the lipid bilayer is transient (the diffusion of cholesterol-anchored DNA alone gives a value higher than for other labeled lipids in the same bilayer), and the diffusion coefficient may be artificially high. However, FRAP measures diffusion coefficients of large numbers of vesicles, many of which are continually colliding with each other, and this is expected to reduce the observed diffusion coefficient. We have chosen to measure diffusion by SPT to measure true individual vesicle diffusivity.

(21) Parente, R. A.; Lentz, B. R. *Biochemistry.* **1986**, *25*, 6678–8.

(22) Asakura, S.; Oosawa, F. *J. Chem. Phys.* **1954**, *22*, 1255.

(23) Dinsmore, A. D.; Wong, D. T.; Nelson, P.; Yodh, A. G. *Phys. Rev. Lett.* **1994**, *72*, 582–5.

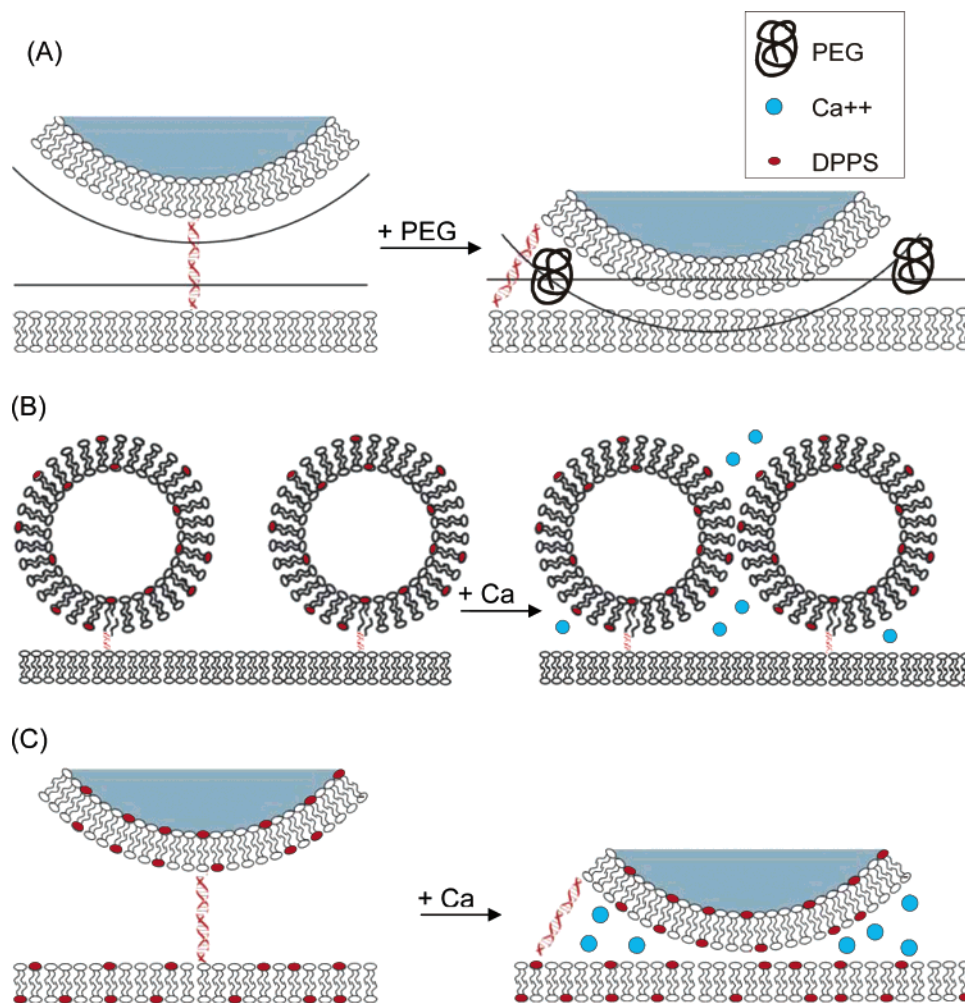


**Figure 5.** (A) Schematic illustration of the depletion effect caused by the addition of a polymer (squiggle) to a tethered vesicle assembly. (See also Figure 4 and movie 2 in Supporting Information.) (B) Schematic illustration of the possible interactions between tethered vesicles containing negatively charged lipids (red) in the presence of Ca ions (blue). (See also movie 4 in Supporting Information.) (C) Schematic illustration of the possible interactions between tethered vesicles and supported bilayers containing negatively charged lipids in the presence of Ca ions. (See also movie 5 in Supporting Information.) All drawings are approximately to scale for a 100 nm vesicle.

membranes, they are excluded from approaching within a distance of  $R_g$  of the surfaces, where  $R_g$  is the radius of gyration of the polymer molecule. If a tethered vesicle is brought within a distance of less than  $R_g$  from the supported bilayer, then the regions around the two surfaces unavailable to polymer begin to overlap. As water molecules are released from the polymer-depleted region adjacent to the membranes, the volume available to the polymer and the net entropy of the system increase. This phenomenon decreases the distance between the vesicle and bilayer. Thus, the introduction of polymer is expected to enhance frictional coupling or other interactions between the two surfaces, resulting in the observed immobilization of tethered vesicles.

To verify that a depletion effect is responsible for the observed vesicle immobilization, the dependence of the effect on the vesicle size was studied. Vesicles extruded through 30 and 200 nm pores were tethered on separate sides of a microfluidic channel. Upon exposure to PBS containing 1% w/v PEG 8000, the 200 nm vesicles stopped, but 30 nm vesicles continued to diffuse normally. (See movie 3 in Supporting Information.) This is consistent with theoretical models that predict a direct relationship between the vesicle radius and the strength of the depletion effect.<sup>23</sup> Furthermore, the effect should be observed using any polymer that is excluded from the surface of a vesicle because this is not a chemically specific effect. We tested this by exposing vesicles

to Dextran 80K (5% w/v in PBS) and concentrated protein solutions (150–200 mg/mL BSA or ribonuclease in PBS), both of which also resulted in reversible immobilization (data not shown). The implications of this effect for membrane interactions in vivo may be interesting because the concentration of proteins in the cytoplasm is within the range studied here. In addition, the same behavior is observed when a supporting membrane with no DNA is exposed to vesicles with no DNA in the presence of PEG. This leads us to suggest that the DNA tether does not prevent vesicle-supported bilayer interactions, and this may play a role in the decreased diffusion rate of tethered vesicle with respect to lipids in the bilayer even in the absence of PEG.

The ability to reversibly stop vesicle diffusion by adding and washing away polymer will be useful in future experiments. For example, kinetic studies of tethered vesicle–tethered vesicle interactions are simplified by immobilizing vesicles to count them and then releasing them to diffuse and react further. The dependence of the depletion effect on vesicle size could also be utilized to specifically manipulate certain populations of vesicles. Finally, introducing polymer into the bulk medium during the tethering incubation speeds the process and can thus streamline sample preparation.

**3.3. Effects of Ca Ions on Tethered Vesicle Diffusion.** The addition of Ca ions to vesicles that display negative charges has

been shown to enhance vesicle aggregation in bulk solution.<sup>24</sup> We can insert acidic lipids such as DPPS into the tethered vesicle alone, the supporting bilayer alone, or both. When 10 mM  $\text{Ca}^{2+}$  was added to tethered vesicles containing 10 mol % DPPS, upon collision the tethered vesicles were observed to diffuse in tandem for some time before separating. (See movie 4 in Supporting Information.) Such transient interactions are not observed for identically prepared samples in the absence of  $\text{Ca}^{2+}$ , and the effect is reversed upon removal of  $\text{Ca}^{2+}$  (data not shown). Likewise, no effect is observed when the tethered vesicles do not contain a negatively charged lipid, either when PS is absent or present only in the supporting bilayer. However, when DPPS is present in both the tethered vesicle and the supporting bilayer, the diffusion of vesicles is reduced upon addition of  $\text{Ca}^{2+}$ . (See movie 5 in Supporting Information.)

These effects can be understood as being the result of  $\text{Ca}^{2+}$ -mediated interactions between negatively charged components on the interacting surfaces. These effects are observed only when negatively charged components are present on both surfaces, whether on different tethered vesicles or on the tethered vesicle and supporting bilayer, as illustrated in Figure 5B and 5C. The latter interactions require that there be opportunities for the tethered vesicle to come quite close to the supporting bilayer, and one would expect some interaction to be present even in the absence of  $\text{Ca}^{2+}$ . As with the depletion effect from polymers, these perturbations to diffusion are interesting in their own right and have applications to studies of vesicle-vesicle interactions, and they indicate that the DNA tether does permit interactions between the tethered vesicle and the supporting bilayer. An extension of this reasoning is that interactions between tethered vesicles and the supported bilayer are always present, albeit to a much lesser extent without polymer or  $\text{Ca}^{2+}$ , and that this coupling slows the diffusion of tethered vesicles relative to that of lipids.

### 3.4. Effects of Sticky Defects on Tethered Vesicle Diffusion.

Video microscopy of diffusing vesicles shows that some vesicles appear to become temporarily immobilized. (See movie 6 in Supporting Information.) These observations, as well as observations in other experiments with supported membranes,<sup>25</sup> lead us to believe that there are defect sites on a supported bilayer that may act as weak binding sites to tethered vesicles. Therefore, we wondered whether defect sites that are even smaller and weaker binding, so that they would not be apparent with the time and spatial resolution of our setup, could affect the measured diffusion coefficient without showing anomalous behavior by SPT. To test this hypothesis, we looked at the effect of sticky defects in a Monte Carlo simulation, lattice model of diffusion. Parameters were adjusted so that under defect-free conditions and SPT tracking and analysis parameters similar to those in the experiment the average diffusion coefficient was  $1.0 \mu\text{m}^2/\text{s}$ . Diffusion coefficients generated after the analysis of about 5000 trajectories gave a spread of  $0.32 \mu\text{m}^2/\text{s}$ , which is close to the value predicted by eq 3,  $0.34 \mu\text{m}^2/\text{s}$ , as expected (Figure 6A). We then introduced randomly distributed defect sites such that a particle encountering this site has a 90% probability of being trapped and a 10% probability of escape with each step. The

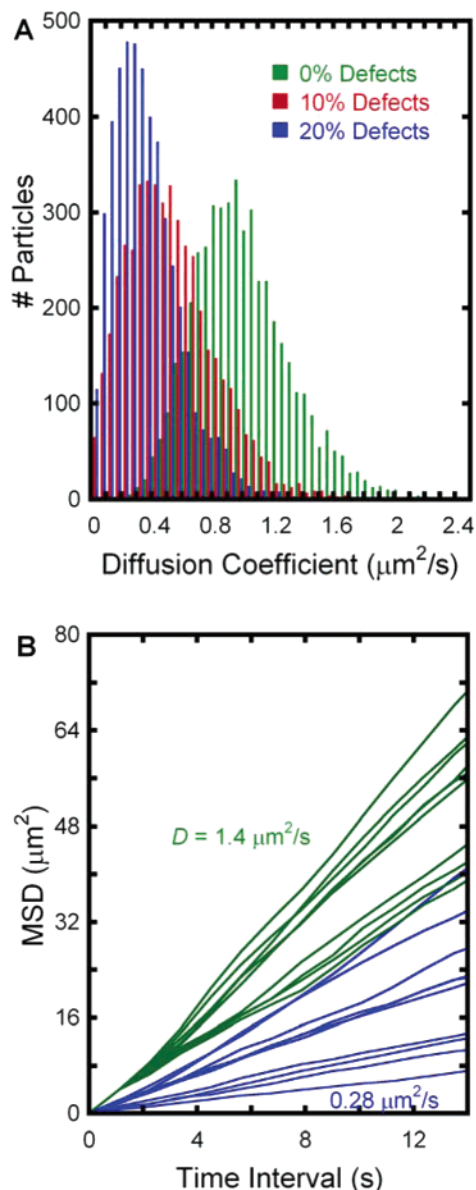


**Figure 6.** (A) Diffusion coefficient distributions from Monte Carlo simulations of randomly diffusing particles on a lattice with varying numbers of sticky defects. Under defect-free conditions, the parameters are set so that the average diffusion coefficient is  $1.0 \mu\text{m}^2/\text{s}$  (green). With 10% surface coverage of sticky defects, the average diffusion coefficient is reduced to  $0.52$  (red) and to  $0.35 \mu\text{m}^2/\text{s}$  (blue) at 20% surface coverage of sticky defects. (B) Example MSD vs time interval plots of defect-free diffusion (green) and 20% sticky defect coverage (blue). In both cases, linear relationships are observed, demonstrating that if such defects exist they cannot be detected as anomalous diffusion with the method of analysis used in our experiments.

system first reached equilibrium by allowing randomly distributed particles to move for 10 000 to 100 000 steps, after which the distribution of diffusion coefficients did not change.<sup>26</sup> At a defect coverage of 10% of all lattice sites, the mean diffusion coefficient was reduced by almost half to  $0.52 \mu\text{m}^2/\text{s}$ , and at 20% defect coverage, the mean was reduced further to  $0.35 \mu\text{m}^2/\text{s}$ . Under these conditions, all particles were observed to interact with defect sites at different points in their trajectories.

Individual SPT trajectories were analyzed by plotting their MSDs as a function of the time interval as shown in Figure 6B. As expected, in the case where no defects are introduced into

(24) Lansman J.; Haynes D. H. *Biochim. Biophys. Acta.* **1975**, *394*, 335–47.

(25) Olson and co-workers showed, by electrophoresis of long DNA molecules electrostatically adsorbed on a cationic supported bilayer, that obstacles existed on the surface of the bilayer that caused DNA molecules to be hooked. (Olson, D. J.; Johnson, J. M.; Patel, P. D.; Shaqfeh, E. S. G.; Boxer, S. G.; Fuller, G. G. *Langmuir* **2001**, *17*, 7396–7401.) If these defects, which are presumably present on our surfaces as well, interact transiently with tethered vesicles, then this could lead to a slowing of the average diffusion as modeled in the text, though the defect density that led to DNA hooking was quite low ( $0.03$ – $0.05 \mu\text{m}^{-2}$ ) so this may be unrelated.

(26) Saxton, M. J. *Biophys. J.* **1996**, *70*, 1250–1262.

the lattice, the relationship is linear (green). However, we also observe normal, linear behavior in cases where random sticky defects are introduced (blue), a result that parallels Saxton's observations in his model of diffusion in two dimensions with reversible binding.<sup>26</sup> These simulations demonstrate that sticky defects that would not be detected can reduce the observed diffusion coefficient and might contribute to our observations.

#### 4. Conclusions

In summary, vesicles tethered on a fluid supported bilayer by DNA hybridization diffuse in the plane of the bilayer, and this diffusion was studied in detail by single-particle tracking. The diffusion coefficients were measured to be 3–5-fold smaller than the diffusion coefficients of fluorescently labeled lipids and DNA–lipid conjugates in the supported bilayer. Indirect evidence suggests that the vesicles are tethered by a single DNA hybridization because no effect on diffusion is observed under conditions where multiple tethers might be formed.  $D$  was insensitive to tethered vesicle sizes from 30 to 200 nm as well as a change in the viscosity of the bulk medium by 3-fold caused by the addition of glycerol. Polymers in solution dramatically slow or halt diffusion, consistent with a depletion effect, suggesting that frictional coupling can occur between the tethered vesicle and the supporting bilayer. Ca ions also reduce diffusion when negatively charged lipids are present in *both* the supporting bilayer and the tethered vesicle, suggesting that the tethered vesicle and supporting membrane can achieve close contact. These results show that tethered vesicle–supported membrane interactions play an important role in determining vesicle mobility.

We reason that, in the absence of mediating agents, transient interactions could contribute to the observed decrease in  $D$  via enhancement of frictional coupling between the two surfaces. Defects in the supported membrane, which reversibly trap diffusing vesicles, can also contribute to the reduced diffusion coefficient compared to that of single lipids, and Monte Carlo simulations show that a significant reduction in  $D$  can be observed while maintaining normal diffusion behavior on the time scale of our experiments. We presume that both frictional coupling and sticky defects contribute to the overall observed reduction in tethered vesicle diffusion, though there is no simple way to assess their relative contributions quantitatively. The polymer

and Ca ion effects can be exploited along with electrophoresis<sup>7</sup> to control the diffusion and lateral organization of tethered vesicles for studies of vesicle–vesicle interactions. This will be described in future publications.

**Acknowledgment.** We thank Dr. Tom Treynor for help with trajectory analysis automation. C.Y.-I. has been supported by Natural Sciences and Engineering Research Council of Canada postgraduate fellowships, the Gabilan Stanford Graduate Fellowship, and the McBain Fellowship in Chemistry. This work was supported in part by grants from the NSF Biophysics Program, NIH GM069630, and by the MRSEC Program of the NSF under award DMR-0213618 (CPIMA). P.L. acknowledges support from the DAAD.

**Supporting Information Available:** Movie 1: Video microscopy of a collection of individual tethered vesicles ( $0.5\times$  real time, 100 nm Texas Red DHPE-labeled tethered vesicles on an egg PC/2% DPPS bilayer,  $5\ \mu\text{m} \times 5\ \mu\text{m}$  field of view) demonstrating 2D diffusion and reversible collisions. Movie 2: Video microscopy of tethered vesicles under two-lane flow in a microfluidic device. Initially, all vesicles diffuse normally. Then, flow is initiated by simultaneously adding PBS to the right lane and PBS + PEG to the left lane. Vesicles in the right lane are carried in the direction of flow, while vesicles in the left lane exhibit highly reduced diffusion. Movie 3: Video microscopy of 200 and 30 nm tethered vesicles exposed to PEG. The larger vesicles on the left exhibit a brighter signal than the smaller vesicles on the right. The entire sample is under PBS + PEG with no flow. Larger vesicles do not diffuse because they experience a greater depletion effect, while smaller vesicles continue to diffuse normally. Movie 4: Video microscopy of a transient tethered vesicle–tethered vesicle interaction mediated by  $\text{Ca}^{2+}$ . Tethered vesicles contain 10% DPPS. During the movie, two tethered vesicles in the circled region will collide and then diffuse in tandem for a short period before separating again. Without  $\text{Ca}^{2+}$ , collisions are completely reversible. Movie 5: Video microscopy of tethered vesicles containing 1% TR and 10% DPPS diffusing on a supported bilayer also containing 10% DPPS. The top half was taken with no  $\text{Ca}^{2+}$  in the bulk medium, and the lower half was taken after the addition of 100 mM  $\text{Ca}^{2+}$  to the bulk medium. Movie 6: Video microscopy of diffusing tethered vesicles transiently sticking to a surface defect ( $0.5\times$  real time, 100 nm Texas Red DHPE-labeled tethered vesicles on an egg PC/2% DPPS bilayer,  $9.3\ \mu\text{m} \times 6\ \mu\text{m}$  field of view). Although these events are relatively rare, there may be smaller sticky defects that lead to a reduction in the average diffusion of tethered vesicles as modeled in the text. This material is available free of charge via the Internet at <http://pubs.acs.org>.

LA0534219